GEOPHYSICAL RESEARCH LETTERS, VOL. 28, NO. 14, PAGES 2731-2734, JULY 15, 2001

Influence of the earthquake cycle and lithospheric rheology on the dynamics of the Eastern California shear zone

Malservisi R. and K. P. Furlong

Geodynamics Research Group, Penn State University, PA

T. H. Dixon

RSMAS, University of Miami, FL

Abstract. The Eastern California Shear Zone is bounded by the high heat flow region of the Basin and Range province and the low heat flow region of the Sierra Nevada block. This difference in thermal state influences the rheology of the lower crust/upper mantle, resulting in a viscosity contrast between the two regions. We analyze the effect of such a contrast on the kinematics and dynamics of the shear zone with numerical models. This viscosity contrast drives asymmetric strain accumulation in the upper crust, producing an asymmetric surface velocity field. An additional consequence of this strain pattern is the potential for asymmetric co-seismic displacement during an earthquake.

Introduction

Models of surface deformation associated with faulting typically assume either a simple elastic half space rheology, or a layered rheology, with an elastic layer overlying one or more viscous or viscoelastic layers. Most such models assume symmetric rheology for strike slip faults, i.e., the crust and upper mantle on either side of the fault are the same. Here we evaluate a region where this assumption may not be valid, using data from the Eastern California shear zone (ECSZ), part of the Pacific-North America plate boundary. The ECSZ accommodates a significant amount (∼20%) of the relative motion between the Pacific and North America plates in California [*Dokka and Travis*, 1990; *Sauber et al.*, 1994; *Savage et al.*, 1990; *Dixon et al.*, 1995, 2000; *Gan et al*, 2000; *Miller et al.*, 2001]. The 1872 Owens Valley earthquake (estimated magnitude ∼8; [*Beanland and Clark*, 1995]), is also consistent with the idea that significant plate motion is accommodated by the ECSZ. The ECSZ is bounded by the Basin and Range province to the east and the Sierra Nevada/Great Valley block to the west. Heat flow measurements [*Blackwell et al.*, 1998] indicate a relatively sharp transition across the ECSZ with low heat flow on the western side and high heat flow on the eastern side (Figure 1). *Dixon et al.* [2000] showed that this transition coincides with a strong gradient in surface deformation. The implied variation in lithosphere thermal structure influences the rheology of the lithosphere and produces a viscosity contrast across the shear zone at depth. A high viscosity lower crust/upper mantle will be associated with the cold Sierra Nevada side, with corresponding lower viscosity on the Basin and Range side.

Paper number 2001GL013311.
0094-8276/01/2001GL013311$05.00

The model

From surface deformation data alone, it is not possible to constrain uniquely the rheology at depth. To model the asymmetric velocity field across the ECSZ, *Dixon et al.* [2000] used faults in different stages of their earthquake cycle, but assumed essentially symmetric lower crustal rheology (Maxwell viscosity 10^{20} Pa s). However, the heat flow data provide an important additional constraint, and imply an asymmetric viscosity distribution. To analyze the deformation field produced by shear strain in association with a viscosity contrast in the lower crust-upper mantle on either side of the ECSZ, we use the finite element model TECTON [*Melosh and Raefsky*, 1980]. We treat the lithosphere as an elastic layer (seismogenic upper crust) overlying a viscoelastic lower crust and lithospheric mantle. The model domain is 500 km wide (x direction, ∼E-W), 150 km long (y direction, ∼N-S) and 70 km thick (z direction). The elastic layer is 15 km thick and overlies a 55 km thick viscoelastic layer with Maxwell (linear) rheology. The far field boundary conditions are a relative velocity of 12 mm/yr (consistent with GPS observations) applied along the sides of the model in a direction parallel to the fault. The top and the bottom surfaces of the model (z=0 and z=70 km) have an imposed boundary condition of no vertical displacement. Slippery nodes [*Melosh and Williams*, 1989] are used to simulate a fault oriented along the y direction in the elastic layer. The fault passes through the center of the model and can be locked to different depths. Although the Eastern California shear zone comprises a complex network of faults [*Reheis and Sawyer*, 1997], the resolution of our mesh does not allow us to study the effects of fault interactions, thus we aproximate this complex fault system as a single master fault.

We consider two model rheologies. In the first, there is no contrast in the viscosity of the viscoelastic layer across the ECSZ (the viscosity of both the Sierra Nevada and Basin and Range regions is set to 10^{19} Pa s). In the second, the viscoelastic layer is divided into two regions with different viscosities. The boundary separating the two regions passes through the center of the model along the plane defined by the fault. The east side simulates the Basin and Range with a low viscosity (10^{19} Pa s) while the west side represents the Sierra block with a higher viscosity (10^{21} Pa s). These

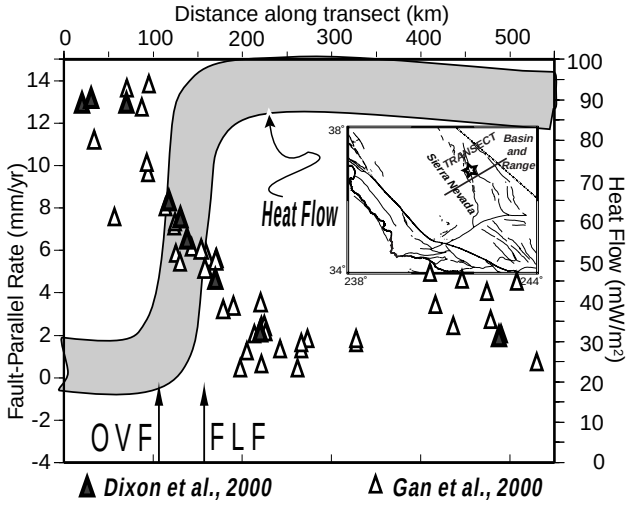

Figure 1. Fault-parallel velocity and average heat flow (http://www.smu.edu/∼geothermal) along an ECSZ transect across Owens Valley (dark line). GPS data from Dixon et al. [2000] (dark triangles) and Gan et al. [1999] (light triangles). Data are projected from up to 50 km away onto the profile. Data uncertainties are slightly larger than symbols. OVF and FLF are Owens Valley and Fish Lake Valley fault zones. Star indicates epicenter of the 1872 Owens Valley earthquake.

viscosities are compatible with the *Lachenbruch and Sass* [1978] thermal profiles and dislocation creep of olivine [*Rutter and Brodie*, 1988]. The effect of the 1872 Owens Valley earthquake is simulated by an applied displacement on the two sides of the locked fault (split node method, [*Melosh and Raefsky*, 1981]) during one time step in the model. In this way, we can produce and monitor post-seismic strain transients consistent with the macro-scale behavior of the earthquake.

Steady state behavior

Steady state deformation models are used to explore the effects of the viscosity structure on the background deformation behavior. We analyze the two end member behaviors of locked/free creeping faults. The shear strain resulting from the model with no viscosity contrast across the ECSZ (homogeneous model) is symmetric with respect to the fault plane. The shear strain is diffuse in the case of a locked fault and more concentrated below the creeping area for a freely creeping fault, consistent with previous analysis (e.g., *Verdonck and Furlong,* [1992]). This strain pattern produces a symmetric surface velocity field (Figure 2). When we introduce a contrast of viscosity in the viscous layer (the contrast model), a significant difference in strain and velocity is seen. In both cases (free fault and locked fault), the shear strain is concentrated in the "weak" material representing the Basin and Range. Coupling of the viscoelastic layer to the elastic layer will lead to an asymmetric deformation at the surface: the largest gradient in the surface velocity field is shifted to the Basin and Range side as compared to the non-contrast model (Figure 3).

Post-earthquake transient

The 1872 strike-slip Owens Valley earthquake (with an estimated magnitude ∼8) had an average surface slip of 6m over a 100km long rupture [*Beanland and Clark*, 1995] (star in Figure 1). To simulate this event and to study the post-seismic transient behavior we locked the nodes on the fault plane to a depth of 5 km for 1000 yr and then imposed a differential slip of 6m on the fault during one time step (1 yr). Figure 2a shows the fault-parallel velocity field for the homogenous model (along a transect perpendicular to the fault) at a set of times after the simulated earthquake. As expected, the post-seismic transient shows a symmetric pattern decaying with the time and essentially reaching steady state after ∼400 yr. Figure 2b shows the history of displacement with respect to the initial position of 7 points at the surface on a transect passing through the center of the studied block. The increasing divergence of the lines graphing the displacement of the surface points indicates internal deformation proportional to the elastic shear strain accumulated by the elastic layer. The contrast of viscosity in the viscoelastic layer introduces asymmetry in the system, and the post-seismic transient is no longer symmetric (Figure 3a). On the Sierra Nevada side, the perturbation

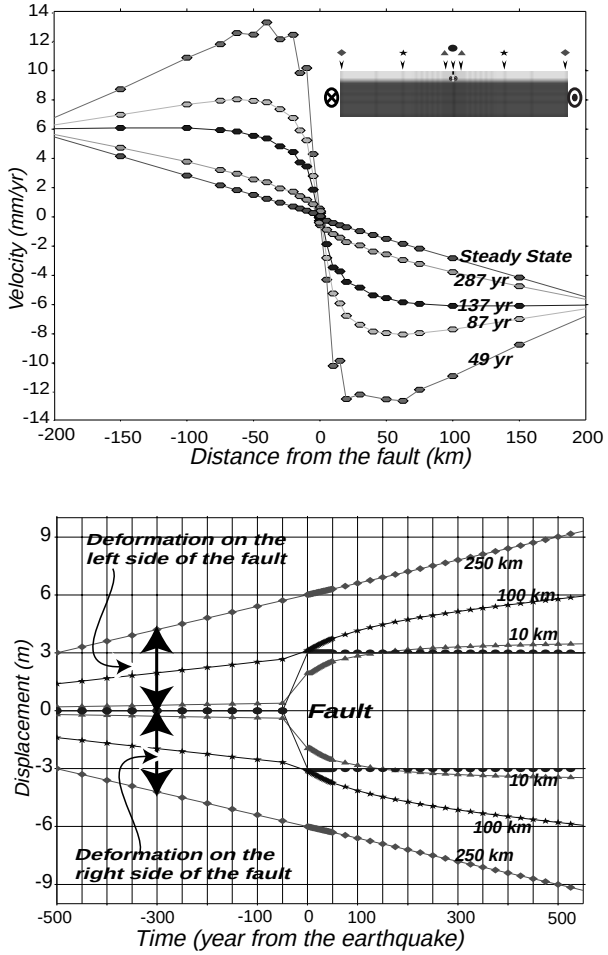

Figure 2. A: predicted fault-parallel velocity field without a viscosity contrast. Curves show different times after the 1872 earthquake. "Steady state" corresponds to the velocity field immediately before the event. B: history of surface displacement with respect to the initial positions of the 7 points at the surface of the model as indicated in figure 2a (Inset). Time 0 corresponds to time of simulated earthquake. Labels on curves show distance from fault. 250 km curves represent motion of points on model boundary and have imposed velocity of (6 mm/yr).

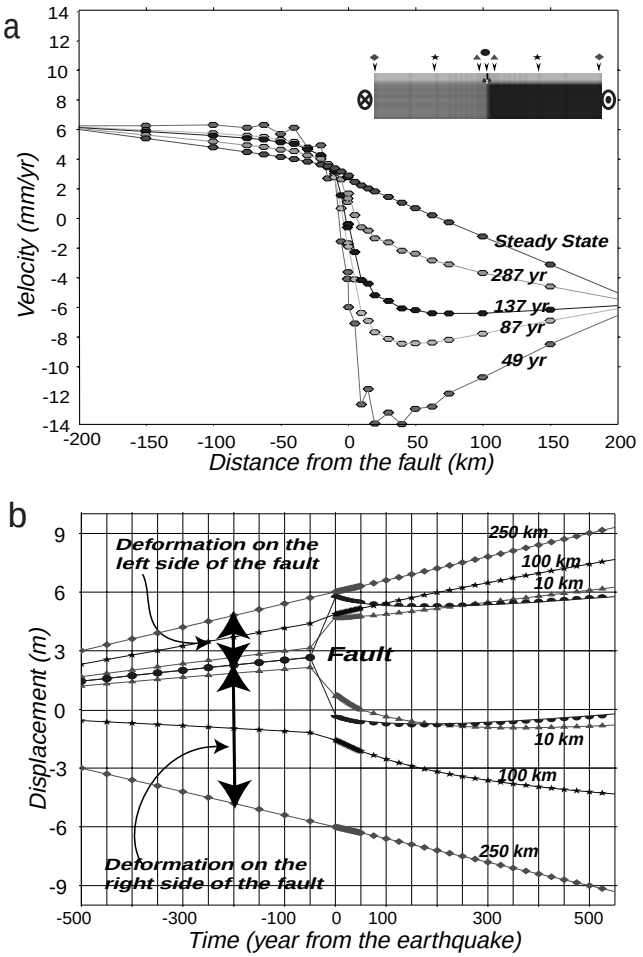

Figure 3. Model results for viscosity contrast in the vicoelastic layer. The figure uses the same notation as figure 2. A: fault-parallel velocity field at different time steps. B: history of displacement with respect to initial position of 7 points at the surface of the model indicated on the inset. Note asymmetric surface deformation field at steady state.

of the fault-parallel velocity field with respect of the steady state is much smaller than the perturbation on the "weak" Basin and Range side. As expected, the smaller deformation on the "strong" Sierra side leads to a faster recovery to the steady state, with a longer transient in the "weak" region. Incidentally, this asymmetric post-earthquake transient indicates that in regions with complex rheologies or geometries, attempts to correct the observed GPS data to remove the earthquake effects must be done prudently. The displacement history (with respect of the original position) of 7 points at the surface (Figure 3b) differs from the no-contrast model. During the period prior to the earthquake, points on the western side of the fault move almost parallel to each other (i.e. the Sierra block behaves almost as a rigid block with little internal deformation). However, the displacements of points on the eastern side (Basin and Range) significantly diverge from the western points. This indicates that the deformation is dominantly on the "weak" side. Interestingly, because of different rates of viscous relaxation in the different parts of the model during the post-earthquake period, there is a time when the results for the homogeneous and the contrast models are practically indistinguishable (in our case around 280 yr after the event). Figure 4 shows our model results compared with the fault-parallel velocity field measured with GPS. Curves are plotted at three different time steps for the contrast (Figure 4a) and homogenous models (Figure 4b). The contrast model results appear to mimic the pattern of the observed velocities quite well. The velocity field is almost flat for the western side; there is a steep gradient close to the fault with a transition to a gentler slope moving to the east. Although both models can satisfy the geodetic observations within the uncertainties, the homogenous model is inconsistent with the heat flow data.

Discussion

During the pre-earthquake period of strain accumulation in the contrast model, there is a pattern of asymmetric deformation (Figure 3b): the western "strong" side is behaving almost as a rigid block with small deformation; the eastern "weak" side accommodates the majority of deformation. The concentration of the deformation in the "weak" side of the model is compatible with the observation of a higher slip rate observed in the faults east of the Owens Valley fault [*Reheis and Dixon*, 1996] since these faults can be seen as the surface manifestation of shear in the weaker lower crust/upper-mantle. This difference in internal deformation of the two sides implies a difference in shear strain accumulation and thus a difference in the storage of elastic energy. Such a difference in strain accumulation on either side of the

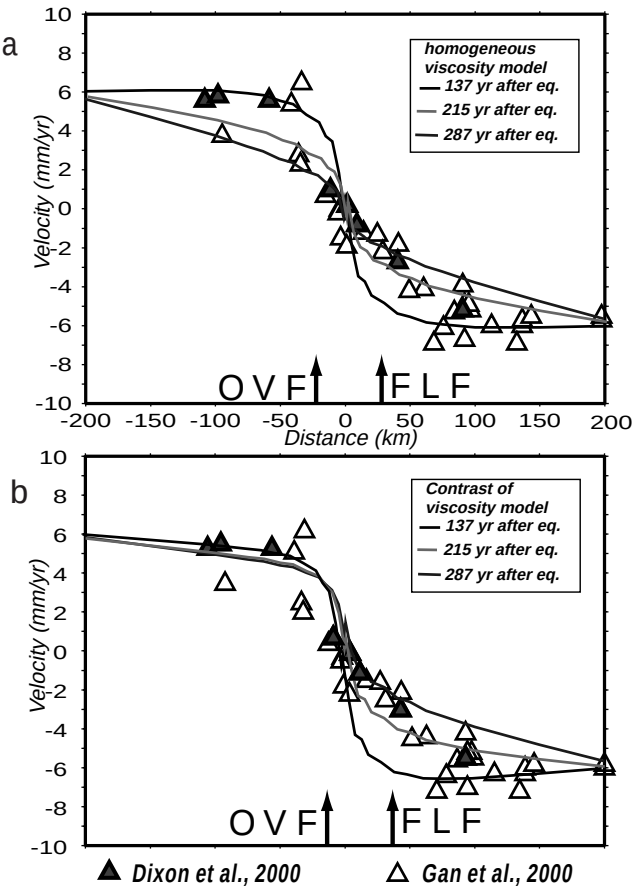

Figure 4. Model predictions without (a) and with (b) viscosity contrast at 3 different time steps. Data and faults shown as in Figure 1.

fault should be reflected in significant asymmetries in the co-seismic "rebound" on either side of the fault during an earthquake. Although we have not specifically analyzed the consequences of such an "asymmetric" earthquake, it seems that effects might be observable in the pattern of strain energy release, ground shaking and/or the seismic radiation pattern. Such asymmetric slip on a strike slip earthquake has been observed elsewhere, although it has been explaned with asymetries in the elastic layer. The November 1997 Manyi, Tibet, earthquake ruptured on an E-W striking fault and shows an asymmetric displacement pattern across the fault [*Peltzer et al.*, 1999]. Asymmetric behavior due to a contrast in elastic properties has been previously analyzed by *Sato* [1974], *Rybicki* [1978], and *Mahrer and Nur* [1979].

Acknowledgments. KPF and RM supported under NSF-EAR 97-25187 and NSF-EAR 99-2937 grants.

References

Beanland, S., and M. M. Clark, The Owens Valley fault zone, eastern California, and surface rupture associated with the 1872 earthquake,*U.S. Geol. Sur. Bull. 1982,* 1995.

Bennett, R.A., J.L. Davis and B.P. Wernicke, Present-day pattern of Cordilleran deformation in the western United States, *Geology, 27(4),* 371-374, 1999.

Blackwell, D.D., K.W. Wisian, and J.L. Steele, Geothermal resource/reservoir investigations based on heat flow and ther -mal gradient data for the United States, *http://www.smu.edu/∼geothermal,* 1998.

Dixon, T.H., S. Robaudo, J. Lee and M.C. Reheis, Constraints on present-day Basin and Range deformation from space geodesy, *Tectonics, 14(4),* 755-772, 1995.

Dixon, T.H.,, M. Miller, F. Farina, H. Wang and D. Johnson, Present-day motion of the Sierra Nevada block and some tectonic implications for the Basin and Range Province, North America Cordillera, *Tectonics, 19(1),* 1-24, 2000.

Dokka, R.K., Travis, C.J., Role of the Eastern California Shear Zone in accomodating Pacific-North America plate motion, *Geophys. Res. Lett., 17(9),* 1323-1326, 1990.

Gan , W., J.L. Svarc, J.C. Savage and W.H. Prescott, Strain accumulation across the Eastern California Shear Zone at latitude 36 30'N, *J. Geophys. Res., 105,* 16229-16236, 2000.

Lachenbruch, A.H., Sass, J.H., Models of an extending lithosphere and heat flow in the Basin and Range Province, *Memoir - Geological Society of America, 152,* 209-250, 1978

Mahrer, K.D., A., Nur, Static strike-slip faulting in a horizontally varying crust, *Bull. Seismol. Soc. Am., 69,* 975-1009, 1979.

Melosh, H. J., and A. Raefsky, The dynamical origin of subduction zone topography, *Geophys. J. R. Astron. Soc., 60,* 333-354, 1980.

Melosh, H. J., and A. Raefsky, A simple and efficient method for introducing faults into finite element computations, *Bull. Seismol. Soc. Am., 71(5),* 1391-1400, 1981.

Melosh, H. J., and C. A. Williams, Jr., Mechanics of graben formation in crustal rocks: a finite element analysis, *J. Geophys. Res., 94,* 13961-13973, 1989.

Miller, M. M., D.J. Johnson, T.H. Dixon, R.K. Dokka, Refined kinematics of the Eastern California Shear Zone from GPS observations, 1993-1998, *J. Geophys. Res., 106,* 2245-2263, 2001.

Peltzer, G., F., Crampe and G. King, Evidence of nonlinear elasticity of the crust from the Mw 7.6 Manyi (Tibet) Earthquake, *Science, 286,* 272-276, 1999.

Reheis, M.C., Dixon, T.H., Kinematics of the Eastern California shear zone; evidence for slip transfer from Owens and Saline Valley fault zones to Fish Lake Valley fault zone, *Geology, 24(4),* 339-342, 1996.

Reheis, M.C., Sawyer, T.L., 1997, Late Cenozoic history and slip rates of Fish Lake Valley, Emigrant Peak, Deep Springs fault zones, Nevada and California, *Geol. Soc. Am. Bull., 109(3),* 280-299, 1997.

Rutter, E.H., K.H., Brodie, The role of tectonic grain size reduction in the rheological stratification of the lithosphere, *Geol. Rund., 77,* 295-308, 1988.

Rybicki, K., Static deformation of a laterally inhomogeneous halfspace by a two-dimensional strike-slip fault,*J. Phys. Earth, 26,* 351-366, 1978.

Sato, R., Static deformations in an obliquely layered medium. Part 1. Strike-slip fault., *J. Phys. Earth, 22,* 455-462, 1974.

Sauber, J., W. Thatcher, S. Solomon and M. Lisowski, Geodetic slip rate for the Eastern California shear zone and the recurrence time of Mojave Desert earthquake, *Nature, 367,* 264-266, 1994.

Savage, J. C., M. Lisowski, W. Prescott, An apparent shearzone trending north-northwest across the mojave Desert into Owens Valley, *Geophys. Res. Lett., 17,* 2113-2116, 1990.

Verdonck, D., K.P., Furlong, Stress accumulation and release at complex transform plate boundaries, *Geophys. Res. Lett., 19,* 1967-1970, 1992.

R. Malservisi, K.P. Furlong, Geodynamics Research Group Department of Geosciences, Penn State University, 542 Deike Building, University Park, PA, 16802, USA. (e-mail: rocco@geodyn.psu.edu)

T.H. Dixon, RSMAS, University of Miami, 4600 Rickenbacker Causeway, Miami, FL, 33149, USA.

(Received February 27, 2001; accepted April 20, 2001.)